# SYNTHESIS AND CHARACTERIZATION OF NICKEL DOPED BISMUTH FERRITE MATERIALS

Lei Lei Aung[1], Aye Aye Khine[2], Khin Nyo Win[3] and Min Maung Maung[4]

## Abstract

Nickel substituted bismuth ferrites($BiFe_{1-x}Ni_xO_3$; x = 0.1, 0.2, 0.3, 0.4 and 0.5) materials was synthesized using combustion technique. The synthesized material powders were sintered at 900°C for 4 hours. X-ray diffraction technique (XRD)was used to confirm the nano-crystallite structure and phase formation. The particle size was estimated by the full width half maximum (FWHM) of the strongest X-ray diffraction (XRD) peak. The characterization of these materials was analyzed by Fourier Transform Infrared spectroscopy (FTIR). The optical band gap of these materials was also investigated from the transmittance spectrum. The energy band gap $E_g$is in the range of 4.7 eV to 5.1 eV for prepared samples.

**Keywords:** bismuth ferrites; Auto-combustion technique; XRD; crystallite size; FTIR; FWHM.

## Introduction

Transition metal oxides constitute one of the most interesting classes of solids, exhibiting a variety of structures and properties. The rich and novel behavior of transition metal oxides arises from the complex interactions between their charges, orbital, spin and lattice degrees of freedom. The interactions in these materials can be modified through the effect of local symmetry breaking, charge transfer, electrostatic coupling and frustrations leading to fascinating new phenomena. The magnetic and ferroelectric orders also couple with each other such that the magnetic degree of freedom can be manipulated by an electric field and ferroelectric degree of freedom by magnetic field. The magneto-electric coupling (ME) in multiferroics promises important technological applications in several multifunctional devices like data storage, spinotronics, sensor and actuator devices etc. Perovskite structure possesses high structural flexibility; a vast number of different but closely related structures can be prepared with the general chemistry $ABX_3$. Doping leads to further ways to chemically tune structural and physical properties.

Bismuth ferrite is one of multiferroic systems showing a large magneto-electric coupling in single phase at room temperature. It is one of the most promising lead- free piezoelectric materials exhibiting multiferroic properties at room temperature. $BiFeO_3$ crystallizes in a distorted rhombohedral perovskite with space group *R*3c. This crystal structure transforms to pseudocubic structure by adding adoping such as Pb, Ba, Ca and Sr. The transformation of crystal symmetry affects multiferroic properties in $BiFeO_3$. Ferroelectricity in $BiFeO_3$ comes from existence of $Bi^{3+}$lon pairs on 6s orbital creating dipolar moment, while anti-ferromagnetism comes from the $Fe^{3+}$ site through anti-ferromagnetic coupling of two adjacent crystal planes. Both $Bi^{3+}$ and $Fe^{3+}$play the major role in the origin of multiferroicity in$BiFeO_3$, then substitution on A and/or B siteenhance its multiferroic properties.

[1] Dr, Associate Professor, Department of Physics, Yangon University of Distance Education.
[2] Dr, Associate Professor, Department of Physics, Yangon University of Distance Education.
[3] Dr, Associate Professor, Department of Physics, Dagon University.
[4] Dr, Associate Professor, Department of Physics, University of Yangon.

In $BiFeO_3$ structure $FeO_6$ octahedron form a basic module which play a major role in determining the properties. The substitutions at Bi-sites are indirect to environment of $FeO_6$ octahedron structure whereas Fe-site substitutions directly affect the octahedron structure. The substitution at both A site and B site simultaneously is supposed to compensate the distortions/strain produced in the structure formation of pure phase materials. Therefore multiferroics are rare and it exhibits weak magnetism at room temperature. As for $BiFeO_3$ bulk ceramic is concerned, synthesis of single phase material is difficult because of the volatility of bismuth oxide at high temperature. The kinetics of phase formation most frequently leads to impurity phases such as $Bi_2Fe_4O_9$, $Bi_2O_3$, and $Bi_{25}FeO_{39}$ etc. The presence of undesired secondary phases and formation of cationic/anionic vacancies, it is difficult to observe ferroelectric loop due to low resistivity of the material resulting in large leakage current, low dielectric constant and high loss. Generally this problem can be resolve by doping of cations at the Bi/Fe sites, or/and both Bi and Fe sites of BFO, single phase synthesis or forming solid solution with other perovskite structure.

The objective of the present work was to be studied the effect of nickel substitution on Bismuth ferrite. The structural characterization of these materials was also identified by XRD, SEM and FTIR spectroscopy. The optical energy band gap was also estimated by the aid of UV-Vis spectroscopy.

## Experimental Procedure

### Preparation of the powders

$BiFe_{1-x}Ni_xO_3$;(x = 0.1, 0.2, 0.3, 0.4 and 0.5) powders were prepared bya sol-gel method. Starting materials were bismuth nitrate, ferric nitrate and nickel nitrate. Each of the above chemicals was weighed according to the stoichiometric ratio and dissolved in the deionized water by constant stirring at the temperature 40-50°C. After ensuring no sediments/precipitate, some citric acid was added and the solution was well mixed for 1-2 hrs. The chelated/complexed acqueous solutions were mixed together and kept at about 70°C for 3–4 days with vigorous stirring to form a viscous gel solution. The gel was dried at about 120°C, which was then collected and pulverized in an agate mortar by grinding. The resultant powders were decomposed at 400°C in an oven to remove the organic solvents. The obtained aqueous powder was sintered at 900°C for 4 hrs.

## Results and Discussion

### X-Ray Diffraction Study

X-ray powder diffraction (XRD) was done to check the phase using the $CuK_\infty$ radiation. Figure 1 shows the XRD pattern of the sintered Ni doped Bi ferrites powders. The strongest reflection of (311) plane represent cubic spinel structure. The BFO powders contained secondary phases such as $Bi_{25}FeO_{40}$ and $Bi_2Fe_4O_9$. Some minor phases were also present. Well defined peaks are (200), (111), (311) and (400) of spinel structure can be observed in the XRD patterns. Moreover, peaks related with $NiFe_2O_4$ were still observed in the XRD patterns of BNFO ceramics. The XRD patterns reveal that $BiFeO_3$ substituted at A site and simultaneously substituted $BiFeO_3$, the XRD patterns are more cleaner in comparison to B site substituted samples. This may be due to compensation of strains produced to substitutions at A and B both sites simultaneously. $NiFe_2O_4$ consumed some Fe, resulting in the excess of Bi in the samples

and therefore increase the formation of the Bi-rich phase, $Bi_{25}FeO_{40}$.The formation of $BiFeO_3$ decrease with increasing of Ni substitution. The XRD patterns of 1 mol% Ni-doped BFO samples (x = 0.1), a pure phase was found. For the 3 mol% Ni-doped BFO (x = 0.3), the above two impurity phases appeared. In the 5 mol% Ni-doped BFO samples (x = 0.5) always contained the Bi-enriched intermediate phase, suggesting that the Ni doping was certainly over the solubility limit.

Using the broadening reflections of 311 and Scherrer's relation X-ray line, the nano-sized nature of the attained ferrite leads to broadening of the powder XRD peaks. The crystallite size of Ni doped Bi ferrite samples was calculated. $D = k\lambda/\beta cos\theta$ where $\lambda$ is the wavelength of the X-ray radiation (1.5406Å), k is a constant taken as 0.89, $\theta$ is the diffraction angle and $\beta$ is the full width at half maximum (FWHM), the crystallite size was found to be varied from47.7 nm to62.9 nm.
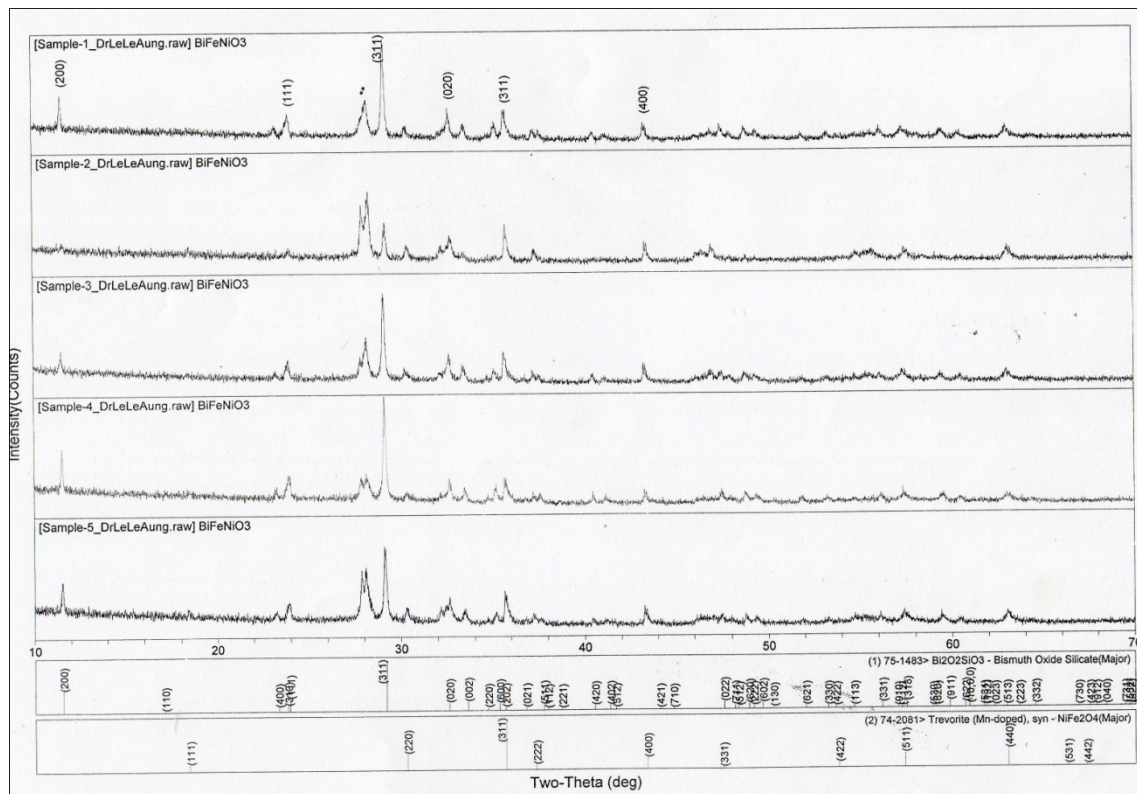


**Figure 1** The XRD pattern of the sintered Ni doped Bi ferrites powders

**Table 1 Lattice parameters, FWHM and crystallite size of $BiFe_{1-x}Ni_xO_3$**

| Prepared samples | a = b = c (Å) | FWHM | Crystallite size (nm) |
|---|---|---|---|
| $BiFe_{0.9}Ni_{0.1}O_3$ | 9.2846 | 0.163 | 49.7 |
| $BiFe_{0.8}Ni_{0.2}O_3$ | 8.2496 | 0.129 | 62.9 |
| $BiFe_{0.7}Ni_{0.3}O_3$ | 7.7995 | 0.170 | 47.7 |
| $BiFe_{0.6}Ni_{0.4}O_3$ | 9.3026 | 0.164 | 49.5 |
| $BiFe_{0.5}Ni_{0.5}O_3$ | 10.0177 | 0.170 | 47.7 |

**TGA-DTA Analysis**

Figure2shows the thermo gravimetric analysis (TGA) trace of Ni doped $BiFeO_3$ samples. The decomposition process consists of three regions. They are 50–150°C, 150–480°C and 480–600°C. Owing to the initial breakdown of the complex and spontaneous combustion, the first weight loss region from 50–150°C indicates the evaporation of absorbed water. With the liberation of $H_2O$, $CO_2$ and$NO_3$ and the nitrate ions providing an oxidizing environment for the combustion of the organic components, the spontaneous combustion is caused from the interactions of ethylene glycol, citrate and nitrate ions in the gel. The second weight loss region observed between 150°C and 480°C is ascribed to dehydration of OH group in the spinel structure of some constituents such as $NO_3$, that lead to two degradation systems involving both inter and intra-molecular transfer reaction, the oxidation of complexes and formation of semi-organic carbon metal/metal oxide. The third weight loss region in the temperature range of 480–600°C is believed to be due to the formation of corresponding metal oxide and the spinel phase. From this study, it is seen that the TGA curve is steady, demonstrating the absolute volatility of water, organic compound, nitrates in the composites, the completion of crystallization route and the immediate formation of pure nickel ferrite.
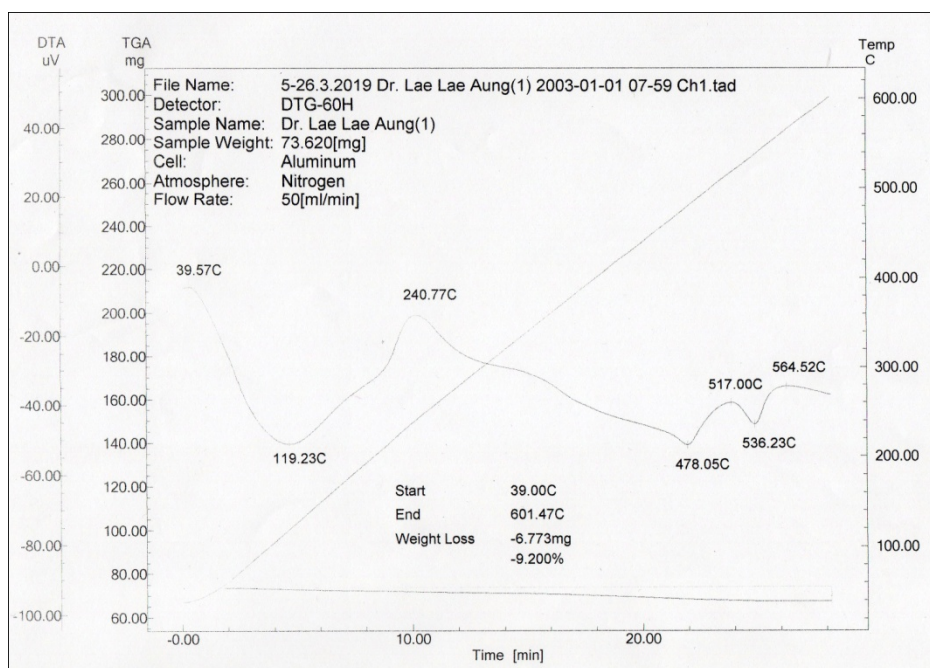


**Figure 2** The thermogravimetric analysis (TGA)  and Differential Thermal Analysis (DTA) of Ni doped $BiFeO_3$ samples
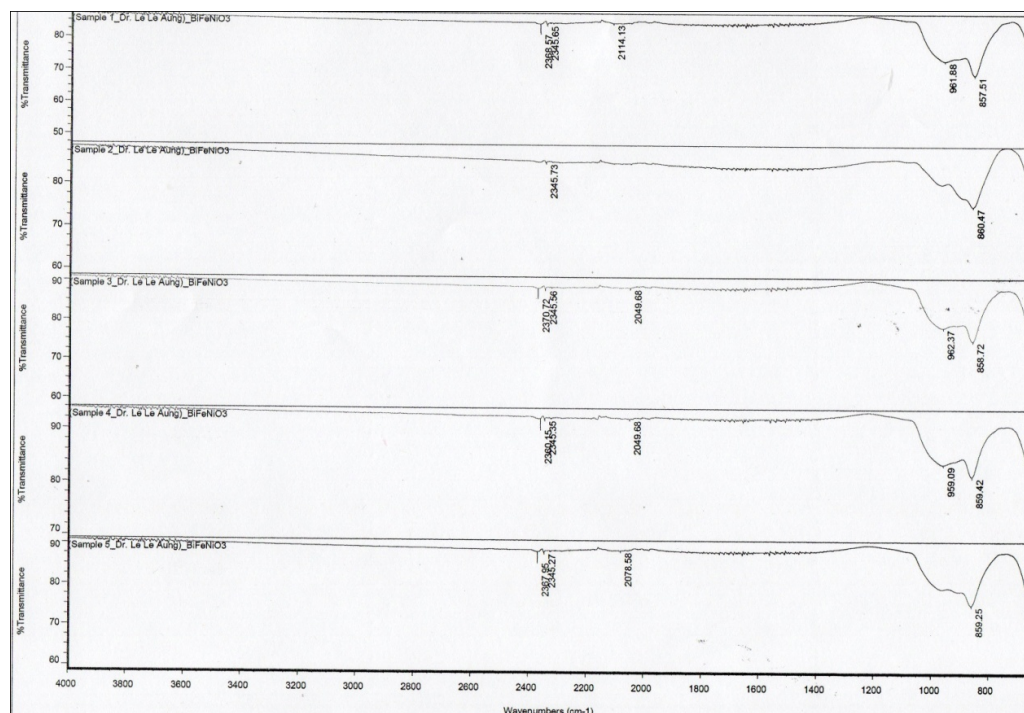
**SEM analysis**

The morphologies of the samples were observed by the scanning electron microscopy (SEM). Figure 3 shows the SEM images of nickel substitution in the bismuth ferrite samples. It was observed that surface of the images was appeared roughly not a smooth surface. The compact sample revealed that the heterogeneous grain size distribution. The surface morphology showed that the shape of the synthesized material approximately uniform in micron size determined by line intercepts method. Moreover, it was observed that the grain size decreases with the increase of nickel substitution in the bismuth ferrite.
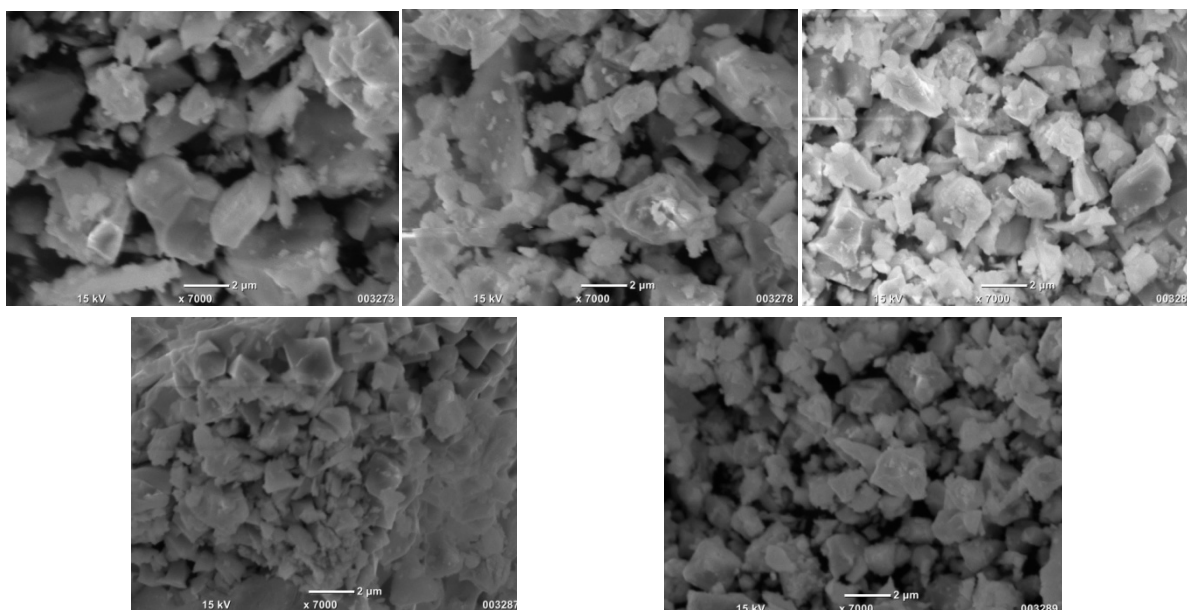
**Figure 3**  The SEM image of Ni doped $BiFeO_3$ samples

## FTIR Analysis

Figure 4 shows the FTIR spectra of prepared samples. The plot shows some distinct peaks. The strong absorption peaks around 400-600 $cm^{-1}$ are attributed to the Fe–O stretching and bending vibrations which are fundamental absorptions characteristics of $FeO_6$octahedral group in the perovskite structure. The formation of perovskite structure can be confirmed by the metal oxygen band. The band at 1387.52 $cm^{-1}$ is due to the presence of trapped nitrate. Typical band characteristics of oxygen metal bonds were observed in the 450-640 $cm^{-1}$ region. A distinct change is noticed that the both side nickel substituted $BiFeO_3$ sample shows two positive peaks near 3000 $cm^{-1}$ compared to the other two compositions. The bands between 3400 and 3784 $cm^{-1}$ could be attributed to the O–H stretching vibration of $H_2O$ absorbed by the sample and the surface O–H or EG. The bands with the peaks at488, 670 and 809 $cm^{-1}$ are assigned to the deformation vibration of Fe–OH groups. The two main metal–oxygen bands at 670 $cm^{-1}$ and 488 $cm^{-1}$ are observed in the FT-IR spectrum of the synthesized Ni doped $BiFeO_3$ samples. These two bands are usually assigned to vibration of ions in the crystal lattices. This indicates the presence of uniformly distributed ferrite particles. The band at 1050 $cm^{-1}$ shows the presence of C–O group vibration modes. At1360 $cm^{-1}$ there is a significant change in the irrelevant peak of –CH bending band. The 1316 $cm^{-1}$ peak is attributed to the characteristic $–CH_3$ bending.

**Figure 4** The FTIR spectrum of Ni dopes BiFeO₃ samples

## Optical Band gap Analysis

The energy band gap of the material is determined by using UV-visible spectra according to Tauc relation $\alpha h\nu = A(h\nu - Eg)^n$, where Egis the energy gap, constant A is different for different transitions, $(h\nu)$ is the energy of the photon and n is an index which assumes the value 1/2, 3/2, 2 and 3 depending on the nature of the electronic transition responsible for the reflection. The value of n is 1/2 for allowed and 2 for forbidden direct energy gap for ferrites. Further, the value of $\alpha$ has been calculated by the following relation, $\alpha = 4\pi k/\lambda$ , where $\lambda$ is wavelength in nm and k is absorption index. Figure 5 illustrated the UV-visible absorbance spectra of the Ni substituted Bi ferrites, the absorbance decreases as the doping of Ni. The value of optical energy band gap $E_g$ has been calculated for the all samples by$(\alpha h\nu)^2$vsh$\nu$plots. The values of $E_g$ for different samples were found by extrapolating the linear portion to the $h\nu$ determine the energy band gap $E_g$to be from 4.7 to 5.1 eV. It was observed that by increasing the concentration of the Ni, the band gap of these materials increased.
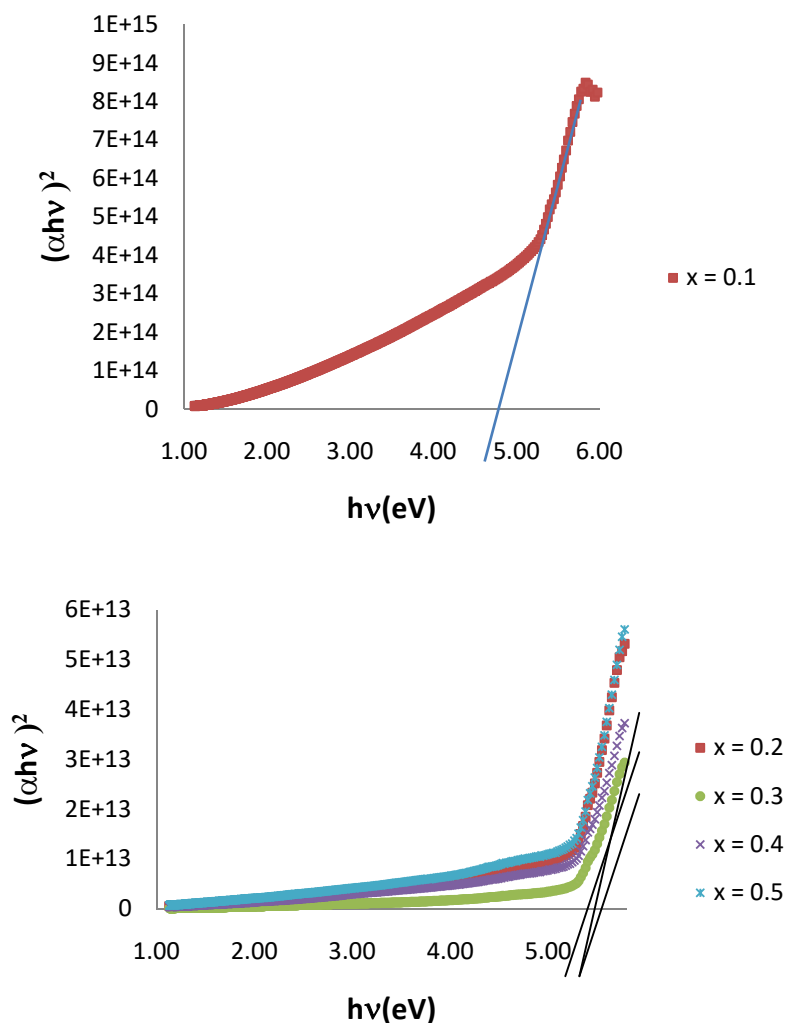
**Figure 5** The energy band gap of Ni dopes BiFeO$_3$ samples

## Conclusion

BiFe$_{1-x}$Ni$_x$O$_3$; (x = 0.1, 0.2, 0.3, 0.4 and 0.5) nano-particles were successfully synthesized by auto combustion method using citric acid as fuel. XRD patterns indicate presence of undesired phases in all samples which get suppressed with simultaneous substitutions on both sites in comparison to substitutions at A-site or B-site in BiFeO$_3$. Ni substitution decreases the formation of BiFeO$_3$, while increase the formation of secondary phases. The Ni substitution has strengthened the magnetic properties of the bismuth ferrite system. The observation of absorption peaks around 400-600 cm$^{-1}$ in FTIR spectra are attribute to Fe-O stretching and bending vibrations and are fundamental absorption peaks of FeO$_6$ octahedron in perovskites. SEM revealed that the synthesized samples have heterogeneous grain size distribution. The energy band gap $E_g$is in the range of 4.7 eV to 5.1 eV for prepared samples.

## Acknowledgement

## References

Ahmad S et al, (2004), "Ferroelectric Ceramics Processing Properties and Applications", Department of Ceramic Science and Engineering, Rutgers University: USA

"Instruction Manual LCR meter GW 820", USA

Moulson A J & Herbert J M, (1997), "Electroceramic Materials Properties Applications", New Delhi: Thomson Press

Suryanarayana C. and Norton M. G. (1998), X-ray Diffraction A Practical Approach, (New York: Plenum)

Tyagi M S, 1991, "Introduction to Semiconductor Materials and Devices", New York: Wiley

Xu Y, 1991, "Ferroelectric Materials and their Applications", New York: Elsevier Science Publishing Co. Inc.